Plasmonics (2010) 5:63–68
DOI 10.1007/s11468-009-9116-0

Photothermal Characterization of Nanogold Under Conditions of Resonant Excitation and Energy Transfer

Santhi Ani Joseph · S. Mathew · Gaurav Sharma · Misha Hari · Achamma Kurian · P. Radhakrishnan · V. P. N. Nampoori

Received: 13 October 2009 / Accepted: 22 December 2009 / Published online: 13 January 2010

Abstract We have performed thermal diffusion measurements of nanofluid containing gold and rhodamine 6G dye in various ratios. At certain concentrations, gold is nearly four times more efficient than water in dissipating small temperature fluctuations in a medium, and therefore it will find applications as heat transfer fluids. We have employed dual-beam mode-matched thermal lens technique for the present investigation. It is a sensitive technique in measuring photothermal parameters because of the use of a low-power, stabilized laser source as the probe. We also present the results of fluorescence measurements of the dye in the nanogold environment.

Keywords Nanogold · Thermal diffusion · Thermal lens · Heat transfer fluids

Introduction

Metallic nanoparticles have been widely used to exploit the local field enhancement due to surface plasmon (SP) and consequent enhancement in a variety of optical processes like nonlinear optical interaction, surface-enhanced Raman scattering (SERS), etc. [1]. Both electromagnetic (EM) as well as chemical mechanisms contribute to the observed enhancement in optical interactions. The former is based on the interaction of the electric field of surface plasmons with the transition moment of an adsorbed molecule, whereas the chemical mechanism is proposed based on the idea that mixing of molecular and metal states can occur. However, studies revealed that the EM mechanism is the important enhancement factor, to which the chemical effect may or may not provide additional enhancement. However, for certain experiments like SERS, some researchers also proposed the chemical mechanism, providing charge transfer states that provide a resonant Raman mechanism at much lower energies than those available in the free molecule. This is true for molecules that are bound to the surface. The large EM enhancements arise from localized surface plasmon resonances (LSPR) excited on the surface of the metal. This excitation is from the incident light at frequency ω with intensity $\left|\overrightarrow{E}(\omega)\right|^2$ as well as the emission from dye at the Stokes shifted frequency $\omega^{|}$ with intensity $\left|\overrightarrow{E}(\omega^{|})\right|^2$. The overall EM enhancement is thus proportional to $\left|\overrightarrow{E}(\omega)\right|^4$ if the width of the LSPR resonance is large compared to the difference in ω and ω_0, the surface plasmon resonance (SPR) peak [2]. It was shown by some researchers that a nearby metal can alter the lifetime of a fluorophore depending on its distance from the metal, after which there has been tremendous interest in research in this direction. Fluorophores behave identical to oscillating point dipoles. Near-field interactions of the fluorophore with the metal can thus alter the rates of radiation from the dye. These interactions can increase the rates of fluorophore excitation and/or emission. At very close distances (<10 Å), radiative rate

S. Ani Joseph (✉) · S. Mathew · M. Hari · P. Radhakrishnan · V. P. N. Nampoori
International School of Photonics,
Cochin University of Science and Technology,
Cochin 682022, India
e-mail: santhia.a@gmail.com

S. Mathew · G. Sharma · P. Radhakrishnan
CELOS, Cochin University of Science and Technology,
Cochin 682022, India

A. Kurian
Department of Physics, Catholicate College,
Pathanamthitta, Kerala, India

enhancement is observed; at intermediate distances (20–300 Å), energy transfer is the dominant process; and at very large distances (>500 Å), fluorescence oscillations caused by dipole-mirror effects take precedence. In general, the quantum efficiency of energy transfer is inversely proportional to $(r/r_0)^n$ where r is the distance between donor and acceptor and r_0 is the distance between donor and acceptor at which the energy transfer efficiency is 50% the case of dipole–dipole energy transfer. In the case of resonant surface plasmon excitation, a small dipole in the excited fluorophore induces a large dipole in the particle, leading to an enhancement in the energy transfer efficiencies [3]. There is also a report about SP-enhanced random lasing in polymer films containing gold nanoparticles when the wavelength of the SPR maximum coincides with that of rhodamine 6G (Rh6G) emission [4].

In this paper, we report experimental results of photothermal studies of chemically prepared gold nanosol using high-power, 532-nm, continuous-wave (CW) laser. This is close to the SPR of gold that we used for the analysis. The experiments were also done in a mixture of the sol and Rh6G, a dye that has emission peak centered at the SPR of the metal. The objective is to analyze the nature of thermal diffusion of the nanofluid and the effect of various possible energy transfer mechanisms on the overall cooling process. Dual-beam, mode-matched thermal lens (TL) technique was employed for the study. The importance of photothermal process is that, if the presence of the metal alters the fluorescence efficiency of the dye, it is worthwhile to verify whether it is compensated in the thermal decay channel. If so, that will result in enhanced/reduced thermal lens signal and will modify thermal diffusion efficiency. There is considerable research on the application and design of nanofluids as efficient coolants and heat transfer agents.

Theory

It is well known that TL technique is sensitive enough to measure very small (as small as 10^{-8}) refractive index changes across the beam width resulting from a temperature variation of ~10^{-5}°C in liquids. A laser beam can thermally induce such refractive index changes, which is the fundamental principle behind TL spectrometry. Basic experimental technique for a thermal blooming measurement is to employ a focused laser beam of appropriate frequency. This creates an artificial beam waist which is a function of the focal length F, the unfocused beam size, and the excitation wavelength, λ. Heat generated in the region of absorption increases the local temperature, thereby modifying the refractive index and inducing an optical lens, which could be diverging or converging depending on the sign of $\partial n/\partial T$, the temperature coefficient of refractive index of the medium. For most liquids, it is a negative lens indicating that they expand on heating. A TL measurement should be performed either by rapidly opening a shutter located in the path of the pump beam or by giving a single shot of pulse for CW and pulsed pump sources, respectively. The TL develops over a period of time governed by the rise time of the excitation pulse and also characteristic of the thermal time constant of the medium. During this time, if one allows another probe beam to pass through the irradiated region and observes the spot at far field, the spot will increase in size, called thermal blooming. Obviously, this size change in the probe spot enables us to calculate $\partial n/\partial T$ and consequently various photothermal parameters of the sample. Alternatively, instead of measuring the beam spot dimensions, it is more convenient to detect the time-dependent laser beam intensity during the transient heating of the sample. In a mode-matched pump probe collinear geometry, this becomes more practical as we can keep an aperture at the center of the undistorted probe beam, and as the pump is turned on, the divergence of the probe results in a decaying probe beam intensity that can be easily recorded using a suitable photodetector. Essentially, the focal length F of the TL formed in a liquid when a CW laser beam is passed through it at $t = 0$ is give by [5]

$$1/F = \frac{P_{\mathrm{abs}}(\mathrm{d}n/\mathrm{d}t)}{\pi k w^2 (1 + t_c/2t)} \tag{1}$$

Here, P_{abs} is the power absorbed by the liquid; k is the heat conductivity of the liquid; w is the beam radius; and $t_c = w^2\rho c/4k$, where ρ=density and c=specific heat. Power absorbed in the liquid is equal to $P\alpha L$ for small αL where P is the incident beam power, α is the absorption coefficient, and L is the length of the cell. The strength of the lens starts to build up from zero at t=0 to a steady-state value. The above expression is valid at power levels sufficiently low such as not to induce spherical aberration in the thermally induced lens due to large phase shifts. As a rule, excitation power, concentration of the sample, optical path length, etc. should be properly adjusted such that the diverging beam spot is free from aberration rings. Under these conditions, it can be shown that the time-dependent probe beam intensity follows the expression

$$I(t) = I_0\left[1 - \theta(1 + t_c/2t)^{-1} + \frac{1}{2}\theta^2(1 + t_c/2t)^{-2}\right]^{-1} \tag{2}$$

Here, the parameter θ is related to the thermal power radiated as heat, P_{th}, and other thermo-optic parameters of the material as $\theta = P_{th}\left(\frac{\mathrm{d}n}{\mathrm{d}T}\right)\lambda_L k$. Interestingly, a knowledge of P_{th} is not necessary to find out θ as it is related to the thermal lens signal through the expression $I = (I_0 - I_\infty)/I_\infty$ and $\theta = 1 - (1 + 2I)^{1/2}$ where I_0 and I_∞ are the initial

and steady-state signals, respectively. θ can be manually computed from the probe beam trace recorded on the oscilloscope as illustrated in the "Experiment" section. Alternatively, detailed curve fitting of this experimental data to Eq. 2 with t_c and θ as the free fit parameters is also a convenient method. From the t_c thus obtained, we calculate the thermal diffusivity D of the sample as $t_c = w^2/4D$ where w is the beam radius at the sample position.

One important source of error in this method is the uncertainty in the measurements of beam spot size. To eliminate this, we standardized the experimental setup using water as explained in the next section.

Experiment

The excitation source is a 532-nm diode-pumped solid-state (DPSS) CW laser with a maximum power of 150 mW. The power at the sample is suitably adjusted using attenuators so that the probe beam spot is free from aberrations. A 2-mW He–Ne used as the probe is arranged to be collinear with the pump, using a dichroic beam splitter. The two beams are focused into the sample cell such that the beam area at the sample plane is the same for both pump and probe, resulting in a mode-matched TL configuration. Sample was taken in cuvettes of 1-cm and 5-mm path lengths for various sets of measurements. A low-frequency mechanical chopper and a shutter were used as required, either to quickly block the pump or to intensity modulate it, depending on the type of data recorded. For example, if the aim is to optimize the TL experiment, it is desirable to use the chopper and adjust the sample position, aperture position, etc. until the TL peak-to-peak signal is maximum. This also enables one to determine the thermal recovery of the sample. On the other hand, when a time-dependent TL signal is required, one should replace the chopper with a shutter. The TL signal was collected using an optical fiber, positioned at the center of the probe beam spot and connected to a photodetector–digital storage oscilloscope (DSO) system. A filter for 532 nm was used before the detector to remove the residual pump.

Absorption and fluorescence spectra were recorded using a standard spectrophotometer and a fluorimeter, respectively.

Results and discussion

Preparation of gold nanosol

Fifty milliliters of 0.01% $HAuCl_4$ solution is heated to boiling and, while stirring, a few hundred microliters of 1% (by weight) trisodium citrate solution is quickly added to the auric solution. The solution changed color within several minutes from yellow to black and then to red or purple color depending on the size of the nanoparticles. The color change is slower for larger nanoparticles than for small nanoparticles. The amount of citrate solution determines the size of the nanoparticles. The faster the capping of the nanoparticles by the citrate, the smaller are the resulting nanoparticles. The sodium citrate first acts as a reducing agent. Later, the negatively charged citrate ions are adsorbed onto the gold nanoparticles, introducing the surface charge that repels the particles. The average size of nanoparticles is 60 nm with plasmon band at 558 nm [6, 7].

When the dimensions of the metallic nanoparticles are large, the spacing of levels within the conduction band is significantly less than the thermal energy, kT, and the particle exhibits a metallic behavior. When the nanoparticles approach a size at which the increased energy separation due to the quantum confinement effect is more than the thermal energy, an insulating behavior results because of the presence of these discrete levels. However, the energy level separations are still too small to affect the optical properties of metals in the UV to the IR range. In the case of noble metals such as gold, there are two types of contributions to the dielectric constant of the metal: One is from the inner d electrons, which describes interband transition (from inner d orbitals to the conduction band), and the other is from the free conduction electrons. The latter contribution, described by the Drude model, is given as [8]

$$\varepsilon_D(\omega) = 1 - \frac{\omega_p^2}{\omega^2 + i\gamma\omega} \tag{3}$$

where ω_p is the plasmon frequency of the bulk metal and γ is the damping constant related to the width of the plasmon resonance band. It relates to the lifetime associated with the electron scattering from various processes. In the bulk metal, γ has main contributions from electron–electron scattering and electron–phonon scattering, but in small nanoparticles, scattering of electrons from the particle's boundaries (surfaces) becomes important. This scattering produces a damping term γ that is inversely proportional to the particle radius r [4, 9]. This dependence of γ on the particle size introduces the size dependence in the surface plasmon resonance condition. For larger-size nanoparticles (>25 nm for gold particles), higher-order (such as quadrupolar) charge cloud distortion of conduction electrons becomes important. These contributions induce an even more pronounced shift of the plasmon resonance condition as the particle size increases. The position and the shape of the plasmon absorption band also depend on the dielectric constant ε_h of the surrounding medium as the resonance condition is

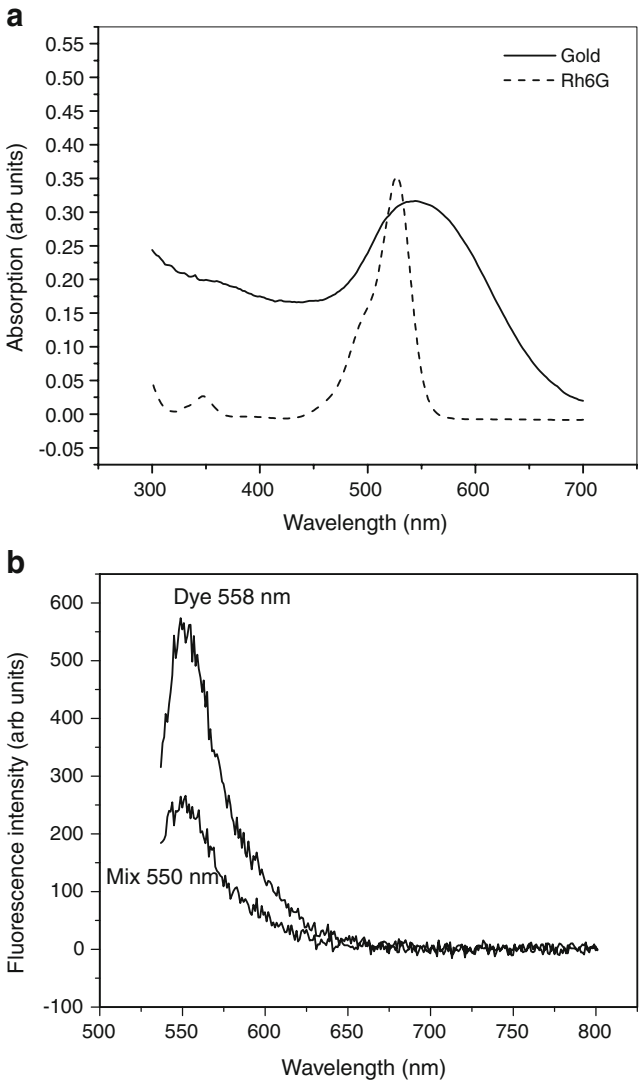

Fig. 1 **a** Absorption spectra of gold nanosol and Rh6G. **b** Fluorescence spectra of Rh6G and a mixture of Rh6G and Au sol

described by $\varepsilon 1 = -2\varepsilon_h$. Hence, an increase in ε_h leads to an increase in the plasmon band intensity and band width, as well as produces a red shift of the plasmon band maximum.

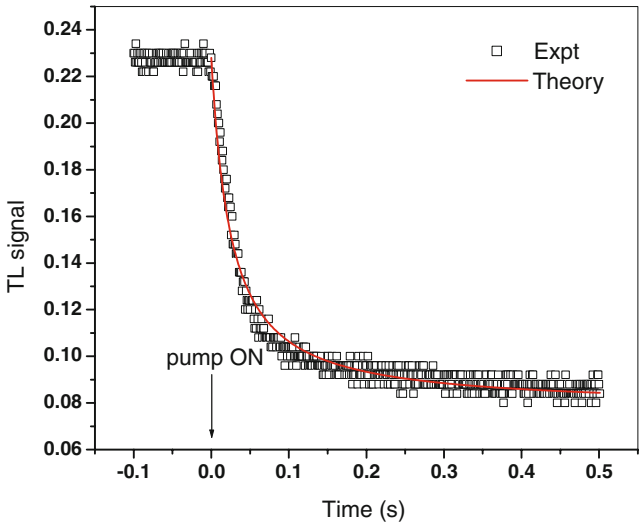

Fig. 3 Typical thermal decay measurement. When the pump is turned on, the probe beam expands. The time constant of this decay is characteristic of the sample

Absorption and fluorescence measurements

Figure 1a shows the absorption spectra of the dye and the gold nanosol. The fluorescence spectra in Fig. 1b reveal that the dye emission is at 558 nm which is the plasmon band of the metal. The addition of the metal has decreased the fluorescence intensity of the dye. The dye emission has contributed to the plasmonic oscillations resulting in lower-intensity fluorescence emission from the mixture. The mixture also shows a blue shift of about 8 nm in the fluorescence peak. Even though the reason is not clear, the dye metal clusters probably occupy a higher vibrational energy level compared to the pure dye resulting in higher-frequency emission.

Photothermal studies

Figure 2 shows the experimental setup for pump probe thermal lens studies. A DPSS laser at 532 nm is used for the excitation. The maximum power delivered by the source is

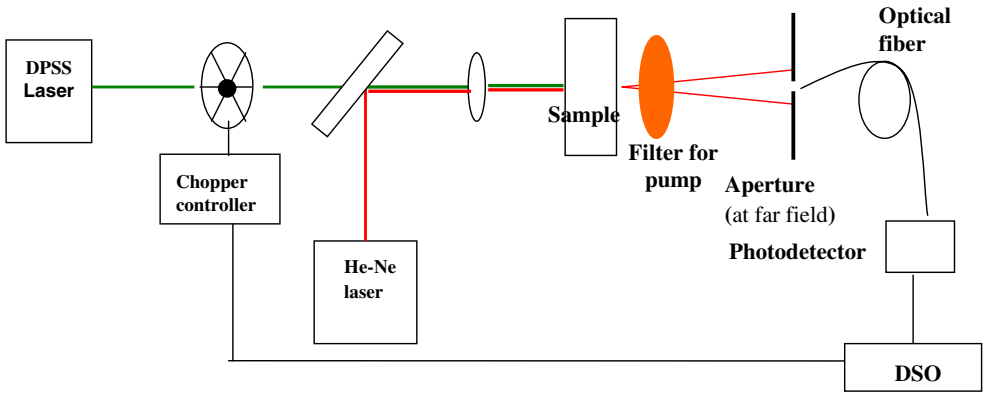

Fig. 2 Dual-beam thermal lens experimental setup for thermal diffusivity measurement

150 mW, CW. It is modulated using a chopper for TL signal measurements. For thermal decay studies, the chopper is replaced by a fast mechanical shutter. He–Ne laser at 2 mW is used as the probe beam. The low intensity ensures that there will not be any photothermal effect due to the probe beam. For the thermal decay measurements, initially, the shutter is closed which blocks the pump and hence there is no thermal expansion. Correspondingly, the probe beam intensity recorded at the DSO is high. When the shutter is quickly opened, there is thermal lens formation, which causes the probe beam to expand. This is illustrated in Fig. 3.

This process is governed by Eq. 2. Fitting the experimental data to Eq. 2 gives the time constant t_c of the thermal decay process. With knowledge of the beam spot size at the sample plane, the thermal diffusivity D can be calculated. The experiment was performed for different concentrations of the gold sol in distilled water and also for various relative volume fractions of the dye Rh6g and gold. Representative graphs of thermal decay are shown in Fig. 4 for gold sol and also its mixture in the dye.

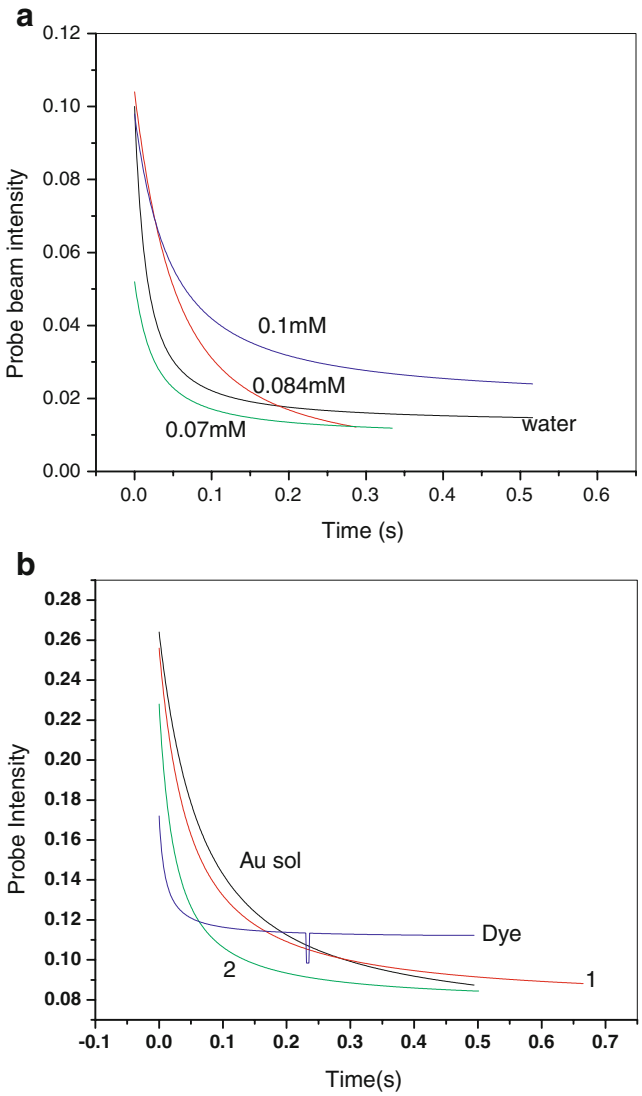

Fig. 4 **a** Thermal lens decay in various concentrations of nanogold in distilled water. **b** Thermal lens decay in various concentrations of nanogold and Rh6G; *1* is gold dye ratio 0.90, and *2* is for the ratio 0.96

Table 1 Data showing time constant and diffusivity of gold dye mixture

Gold/dye	t_c (ms)	D (10^{-2}cm^2/s)
Water	25.5	0.1412
1.0	309.9	0.0116
0.96	193.0	0.0187
0.93	160.4	0.0224
0.90	161.9	0.0222
0.87	92	0.0391
0.84	96.4	0.0373
0.82 at 15 mW	8	0.4500
0.82 at 45 mW	86	0.0419
0.82 at 136 mW	484.4	0.0074
0.82 at 150 mW	1767.4	0.0020

The variation of diffusivity with different relative volume fractions of gold and dye in the mixture and also with concentration in a pure gold sol are shown in Tables 1 and 2, respectively. The sample shows temperature-dependent diffusivity as shown by the last four rows of Table 1 which were performed at different power levels of the pump laser. And, in this case, at the lowest power level, the diffusion is four times larger than that of water, which is a very good indicator of the application of this nanofluid as a coolant. Therefore, for low gold concentrations, the nanofluid is efficient in dissipating low temperature fluctuations in the medium. It can be seen that the heat diffusion mechanisms are not the same for a pure gold solution and the gold–dye mixture. For the former case, the decrease in metal concentration reduces D. Therefore, it can be assumed that collision of the metal nanostructures and their Brownian motion are the major thermal decay channels. Whereas in the presence of dye, energy transfer between the two species,

Table 2 Data showing the diffusivity of gold sol at various concentrations in distilled water

Sample (mM)	Theta	D(10^{-2}cm^2/s)
0.1	−3.0408	0.0225
0.084	−2.0928	0.0222
0.08	−6.1253	0.0201
0.07	−3.6673	0.0184
0.01	−2.9139	0.0165

Theta is a measure of the initial slope of the decay curve

cage formation of the dye around the metal, and the movements of this macromolecules, etc. should be considered. Low temperature fluctuation is dissipated faster. The reason for this can be that high-power laser will induce cluster formation, and the heavy macromolecule will have slower rate of motion and hence smaller *D*. Even in this case, smaller concentration of gold results in better dissipation. The dye molecules get attached around gold and forms a cage-like structure. This reduces the Brownian motion and hence *D*. Therefore, for better results, we should maintain the gold/dye ratio around 0.82 by molar volume.

Conclusion

We have studied the thermal diffusivity of nanogold and its mixture with Rh6G dye at various concentrations using the mode-matched thermal lens method. Generally, the diffusion of gold nanofluid is lower than that of water. However, at certain relative volume fractions of this solution with Rh6G and at low excitation power, the diffusion is four times faster than that of water which will make this kind of fluid as efficient heat transfer agents. We have also observed that the diffusion is temperature dependent. The study will be useful in designing heat transfer nanofluids which will particularly find application in random lasing. Emission from dye molecules will be amplified because of the nanoresonators of gold. The small rise in temperature will be dissipated by the gold themselves.

Acknowledgement Authors acknowledge financial support from the University Grants Commission, India.

References

1. Franzen S, Folmer JCW, Glomm WR, O'Neal R (2002) Optical properties of dye molecules adsorbed on single gold and silver nanoparticles. J Phys Chem A 106:6533–6540
2. McMahon JM, Henry A-I, Wustholz KL, Natan MJ, Freeman RG, Van Duyne RP, Schatz GC (2009) Gold nanoparticle dimer plasmonics: finite element method calculations of the electromagnetic enhancement to surface-enhanced Raman spectroscopy. Anal Bioanal Chem. doi:10.1007/s00216-009-2738-4
3. Ray PC, Darbha GK, Ray A, Walker J, Hardy W (2007) Gold nanoparticle based Fret for DNA detection. Plasmonics 2:173–183
4. Popov O, Zilbershtein A, Davidov D (2006) Random lasing from dye-gold nanoparticles in polymer films: enhanced gain at the surface-plasmon-resonance wavelength. Appl Phys Lett 89:191116
5. Brannon JH, Douglas M (1978) Absolute quantum yield determination by thermal blooming. Fluorescein. J Phys Chem 82:No.6705
6. Kimling J, Maier M, Okenve B, Kotaidis V, Ballot H, Plech A (2006) Turkevich method for gold nanoparticle synthesis revisited. J Phys Chem B 110:15700
7. Frens G (1973) Controlled nucleation for the regulation of the particle size in monodisperse gold suspensions. Nat Phys Sci 20:241
8. Jang SP, Choi SUS (2004) Role of Brownian motion in the enhanced thermal conductivity of nanofluids. Appl Phys Lett 84 (21):4316
9. Kumar DH, Patel HE, Kumar VRR, Sundararajan T, Pradeep T, Das SK (2004) Model for heat conduction in nanofluids. Phy Rev Lett 93:144301